International Journal of Applied Research 2016; 2(9): 493-497

ISSN Print: 2394-7500
ISSN Online: 2394-5869
Impact Factor: 5.2
IJAR 2016; 2(9): 493-497
www.allresearchjournal.com
Received: 11-07-2016
Accepted: 15-08-2016

Susheel Kumar Singh
Assistant Professor,
Department of Physics,
HLY PG College, Lucknow,
Uttar Pradesh, India

Bhuvan Bhasker Srivastava
Associate Professor,
Department of Physics,
Shia PG College, Lucknow,
Uttar Pradesh, India

Correspondence Author:
Bhuvan Bhasker Srivastava
Associate Professor,
Department of Physics,
Shia PG College, Lucknow,
Uttar Pradesh, India

Optical properties of pure polypyrrole and TiO_2 doped polypyrrole

Susheel Kumar Singh and Bhuvan Bhasker Srivastava

Abstract
This present work describes an efficient method to synthesize and characterization of pure PPy and PPy/TiO_2 nanocomposites by one-step in-situ polymerization of Pyrrole. TiO_2 nanoparticles were used as a dopant of PPy because of their excellent physical and chemical properties as well as extensive uses in many areas like coatings, solar cell [1]. The characteristics of the molecular structure, crystalline, optical properties, photoconductivity properties, and morphology of the pure PPy and PPy/TiO_2 nanocomposites are also discussed.

Keywords: Pure polypyrrole, TiO_2, doped polypyrrole

1. Introduction

1.1 Sample Preparation

Pyrrole was distilled before use. All other reagents and solvents obtained from SDL were of reagent grade and were used as received. All solutions were prepared using distilled water, all reactions were conducted at a temperature of 5 °C. The solution of the oxidizing agent, Ammonium persulfate (APS), was prepared using distilled water and was used in the ratio of 1:2.4 (monomer: oxidant). Dopants were mixed with Pyrrole solution (10% w/w) and stirred for 30 minutes for proper mixing and then the oxidant solution was added slowly. The Polypyrrole was prepared by chemical polymerization method by using 0.1M Pyrrole solution prepared by using distilled water and then mixed with an oxidizing agents in the ratio mentioned above. Then the polymerization was conducted for 4 hours under constant stirring. This preparation was kept unagitated for 24 hours so that PPy powder settled down. The PPy powder was filtered out under vacuum and washed with distilled water several times to remove any impurities present. The Polypyrrole was dried for 2 days at room temperature [2]. The pure and TiO_2 mixed PPy composite were grinded in form of fine powder. Pellets were prepared by compressing the powder under a pressure of 10 tons with the help of a hydraulic press machine. All the pellets were annealed at 100 ^{0}C for one hour. The thickness of the pellets sample was found to be 3mm. The diameter of the pellets was found to be 13 mm.

1.2 Measurements

The XRD spectra of all the samples recorded by PANalytical, X'pert PRO diffractometer using CuK_α radiation (λ=1.54056 A^o) were presented for structural analysis of the samples. The SEM images of all the sample pellets were taken by scanning electron microscope (Model-430, LEO Cambridge, England). FTIR spectra of all the samples in the form of powder were recorded on the Bruker Alpha spectrometer to determine the formation of Polyaniline. To record absorbance spectra, 0.02 g of each sample is dissolved in 5mL of m-cresol and then the absorption spectra of the solutions thus formed were recorded with UV–vis spectrophotometer (Model No.V-670 JASCO).

2. Result and Discussion

2.1 XRD Analysis

XRD patterns study of nanocomposites of pure PPy and the synthesized PPy/TiO_2 nanocomposites are presented in Fig.1, the XRD pattern of pure PPy as shown in figure that the in absence of TiO_2 nanoparticles is amorphous.

It can be seen from curves Fig.1(b–d) for the PPy/TiO_2 nanocomposites as the TiO_2 percentage was increased the amorphous nature disappeared and the PPy/TiO_2 nanocomposites samples become more strongly oriented along the (101) direction, which shows for all PPy/TiO_2 nanocomposites samples are polycrystalline nature with tetragonal structure with its most intense peak located at 25.5^0. The angle obtained from the 2θ value corresponding to the (1 0 1) peak, which is attributed to the anatase TiO_2 phase, was used to measure the tetragonal specimen lines [3]. The different peaks in the diffractogram were indexed and the corresponding values of inter planar spacing 'd' were calculated and compared with the standard (JCPDS card no. 89-4921). The main peaks 2θ is around at 25.57^0, 38.15^0 and 48.15^0 corresponding to (101), (004) and (200) planes of PPy/TiO_2 nanocomposites. These similar peaks were earlier reported for the PPy/TiO_2 nanocomposites by M.R. Mahmoudian *et al*. [4]. The structures are found tetragonal at the peaks (0 0 4) and (2 0 0) of the PPy/TiO_2 nanocomposites, similar type of structure was reported for TiO_2 nanocomposites [5]. XRD patterns of PPy/TiO_2 nanocomposites show that the small diffraction peak for the all PPy/TiO_2 nanocomposites samples, it implies that when Pyrrole is polymerized on TiO_2, each phase maintains his initial structure. The intensity of PPy/TiO_2 nanocomposites has been decreased with increased TiO_2 nanoparticles due to the surface coverage of the nanoparticles by PPy [6]. In case of tetragonal crystal structure (a = b ≠ c), the lattice parameter is calculated using the following Lattice Geometry formula: $d_{hkl} = a/\{h^2+k^2+l^2(a^2/c^2)\}^{1/2}$ [7]. Where d_{hkl} is the interplaner separation corresponding to Miller indices h, k, l; a, b and c are lattice parameters. The calculated lattice parameters values corresponding peaks (004) and (200) for the 10, 15 and 20wt%TiO_2 doped PPy such as (a =1.88, c = 4.6), (a = 1.88, c =4.64) and (a = 1.88, c =4.74). The crystallite size of PPy/TiO_2 nanocomposites, calculated by Debye Scherrer's formula $D = K\lambda/\beta\cos\theta$ [8].

Where 'D' is the Grain Size, 'K' is proportionality constant and it is approximately equal to unity, 'β' is the FWHM of the peak in radians (theoretically corrected from the Instrumental broadening), 'θ' is the Bragg's angle, 'λ' is the wavelength of X-rays (1.5406Å for CuK_α). The average crystallite size was found to be about 15 and 24nm respectively.

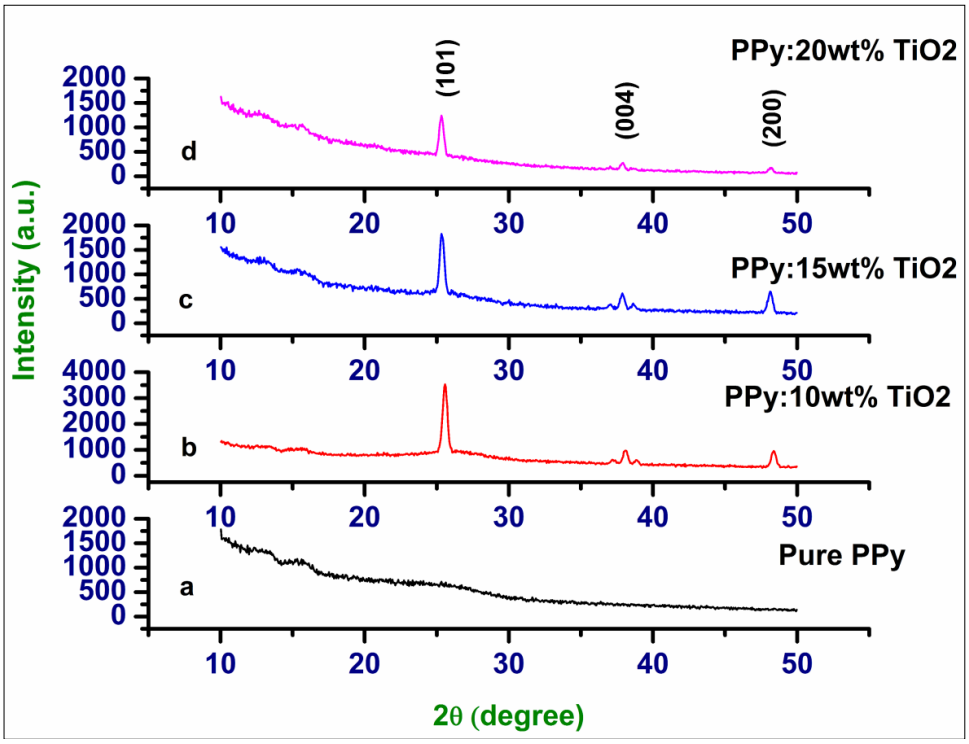

Fig 1: XRD spectra for the sample a, b, c and d and curves a, b, c and d correspond to 0, 10, 15 and 20 wt% TiO_2 doped PPy nanocomposites, respectively.

2.2 Scanning Electron Microscopy

Scanning electron microscope was used to study the surface morphology of the pure Polypyrrole and Polypyrrole doped with various dopant percentage of TiO_2 by chemical oxidation method. Fig.2 (a), (b), (c) and (d) show the sphere shape of nanoparticles. SEM images shown in Fig.2 (b-d) for the PPy/TiO_2 nanocomposites have large nanosphere are due to the introduction of the relatively higher content of TiO_2. We noticed that as the amount of TiO_2 increased the number of pores and size of the pores also increased, which play very important role for conductivity. In contrast, the size of the Polypyrrole nanosphere increases, when the large doping weight percentage were used, the conductivity of these Polypyrrole nanospheres is comparable to that of Polypyrrole nano fibers already reported. That is to say, the initiator molecules act as a stabilizer for the as-formed nano-micelles. These nano-micelles likely act as templates to encapsulate Pyrrole and oxidant leading to the formation of nano-spheres during polymerization.

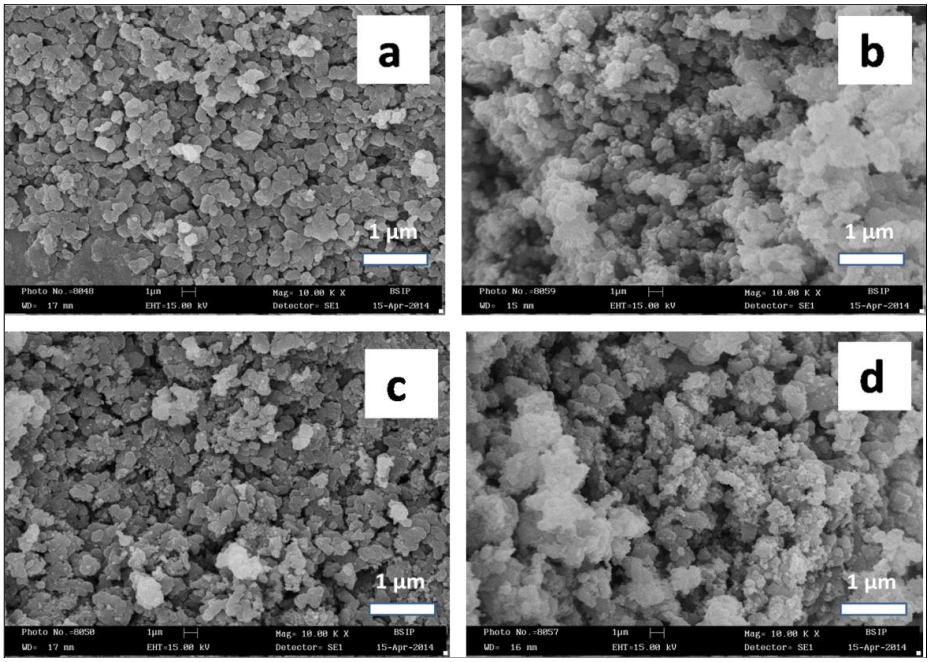

Fig 2: SEM images of samples a, b, c, and d and images a, b, c and d correspond to 0, 10, 15 and 20 wt% TiO_2 doped PPy nanocomposites, respectively.

2.3 FTIR Analysis

The FT-IR transmittance spectra of pure PPy and PPy/TiO_2 nanocomposites are recorded in the range of 400 – 4000 cm^{-1}, which is shown in Fig.3 (a–d). The FTIR spectra are for Polypyrrole and PPy/TiO_2 nanocomposites with different weight percentages of TiO_2. The absorbance bands between of 1400 to 1600 cm^{-1} in the FT-IR spectra of the synthesized Polypyrrole can be attributed to the fundamental vibrations of the Pyrrole rings [9]. The absorbance bands at 770 cm^{-1} and 883 cm^{-1} is attribute of C-H out of plane bending, the absorbance bands at 1175 cm^{-1} and 1044 cm^{-1} is attribute of C-H in plane bending, the absorbance band at 1535 cm^{-1} is attribute of C-N stretching, the absorbance band at 1311 cm^{-1} is attribute of C=C stretching, the absorbance band at 2340 cm^{-1} is attribute of C-H stretching, the absorbance band at 3730 cm^{-1} and 3848 cm^{-1} is attributed of N–H stretching, similar absorbance bands are reported by S. Deivanayayaki *et al.* [10]. A small absorbance band around at 1699 cm^{-1} corresponds to Ti-O-C stretching mode in each case [11]. Fig.3(b–d) of PPy/TiO_2 composites indicate that the N-H, C-H, C=C and C- N stretching are shifted slightly. With the increase of TiO_2 content, the intensity of each peak is found to be decreasing. The FTIR study confirms that the TiO_2 molecules are well incorporated with Polypyrrole structure. The FTIR spectrum of PPy/TiO_2 nanocomposites in Fig.3 (b-d) is similar of the pure PPy spectrum, which shows that PPy chains have been formed in the PPy/TiO_2 nanocomposites.

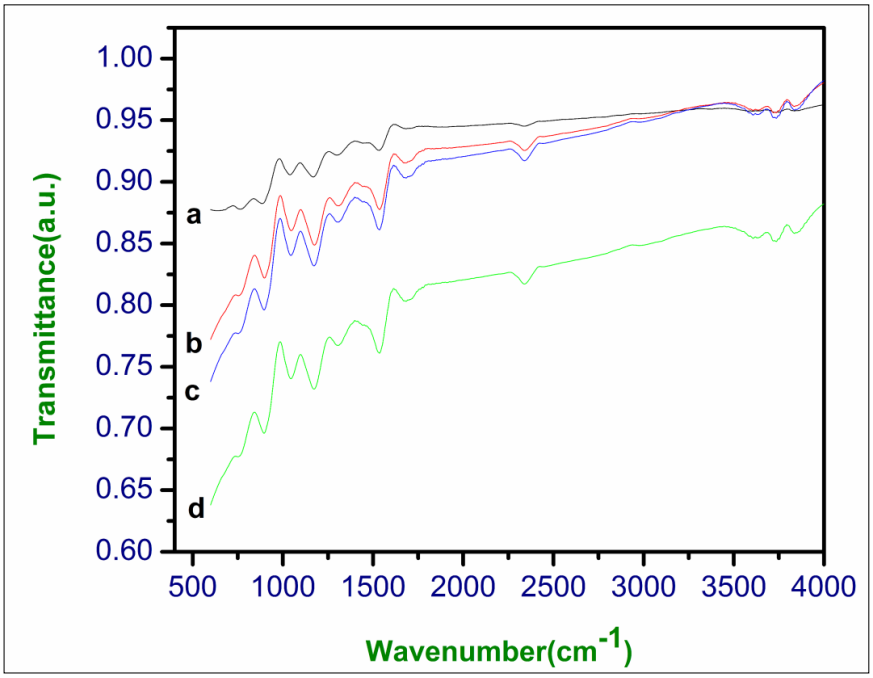

Fig 3: FTIR spectra for the sample a, b, c, and d curves a, b, c, and d correspond to 0, 10, 15 and 20 wt% TiO_2 doped PPy nanocomposites, respectively.

2.4 UV-visible Spectroscopy

The UV–vis absorption spectra of the pure PPy and the PPy/TiO_2 nanocomposites are recorded at room temperature by using a spectrophotometer between the wavelength range 200–800 nm as shown in Fig.4. Optical spectroscopy is an important technique to understand the conducting states corresponding to the absorption bands of inter and intra gap states of conducting polymers [12]. Solution of all PPy and PPy/TiO_2 nanocomposites sample shows the observed peak at 308nm was assigned to the π-π* transition or the excitation transition. As seen in the Fig.4 pure PPy and PPy/TiO_2 nanocomposites as the dopant percentage of TiO_2 increases, the intensity of PPy/TiO_2 nanocomposites increased and the polaron band appears to be sharp peak. This indicates that an increase in the dopant percentage leads to the formation of a chain which forms the best sharp peaks [13]. The differences between the two spectra are due to the presence of an electron-withdrawing sulfonic group in the complex and therefore the transition band is observed at a lower wavelength. The absorption of the polaron band is strongly dependent on the molecular weight of the polymer [14].

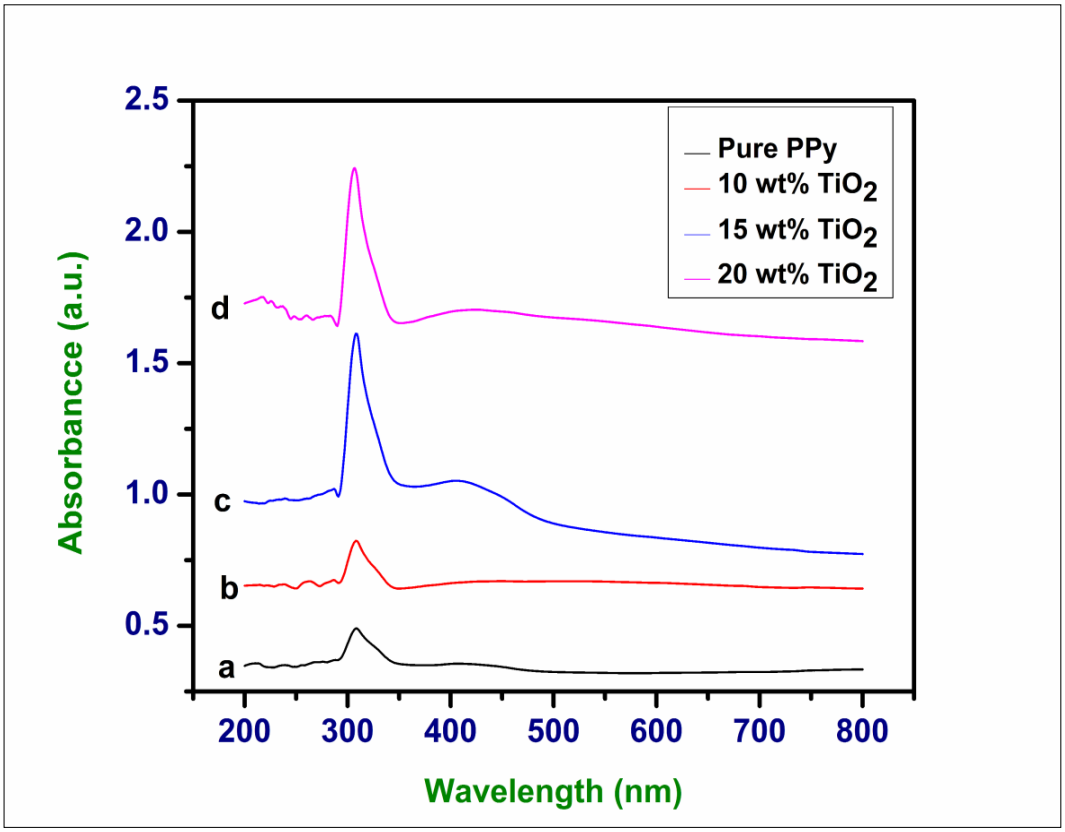

Fig 4: UV–vis absorption spectra for the sample a, b, c and d. Curves a, b, c and d correspond to 0, 10, 15, and 20 wt% TiO_2 mixed PPy nanocomposites respectively.

2.5 Photoluminescence Studies

Photoluminescent organic molecules are new classes of compounds with interesting properties. They undergo emission over a wide range from the violet to the red. They can also be combined in several different forms to produce white light. One category of organic material with photoluminescence properties is conjugated organic polymers. PL spectra were measured for all the four samples in the range of 200 – 700 nm and the wavelength of excitation chosen for all the samples is 325 nm. The photoluminescence spectroscopy (PL) of TiO_2 doped PPY has been performed and is shown in Fig.5. The PL spectra of 0, 10, 15 and 20 wt% TiO_2 doped PPy samples shows one emission peak centered at around 368 nm in ultra-violet region, and two broad visible peaks at around 480 nm in blue region and sharp peak at around 530 nm in green region. The similar related PL peak has been reported for the PL spectra of TiO_2 doped PPy at 362 nm [15]. We also note that an increase in intensity of the 368 nm, which becomes the dominant emission band as the TiO_2 concentration increases.

The band gap of the Pure PPy and PPy/ TiO_2 nanocomposites of different wt% were found to be the corresponding main visible emission peaks as 3.37 eV, 2.58 eV and 2.34 eV. The band gap gets decreased at every emission peaks because the peaks shifted due to increased content of TiO_2 nanoparticles. As the luminescence of these oxide/polymer nanocomposites is proportional to the surface features, it is possible to tailor the wavelength and the intensity of the luminescence by varying the particle size [16].

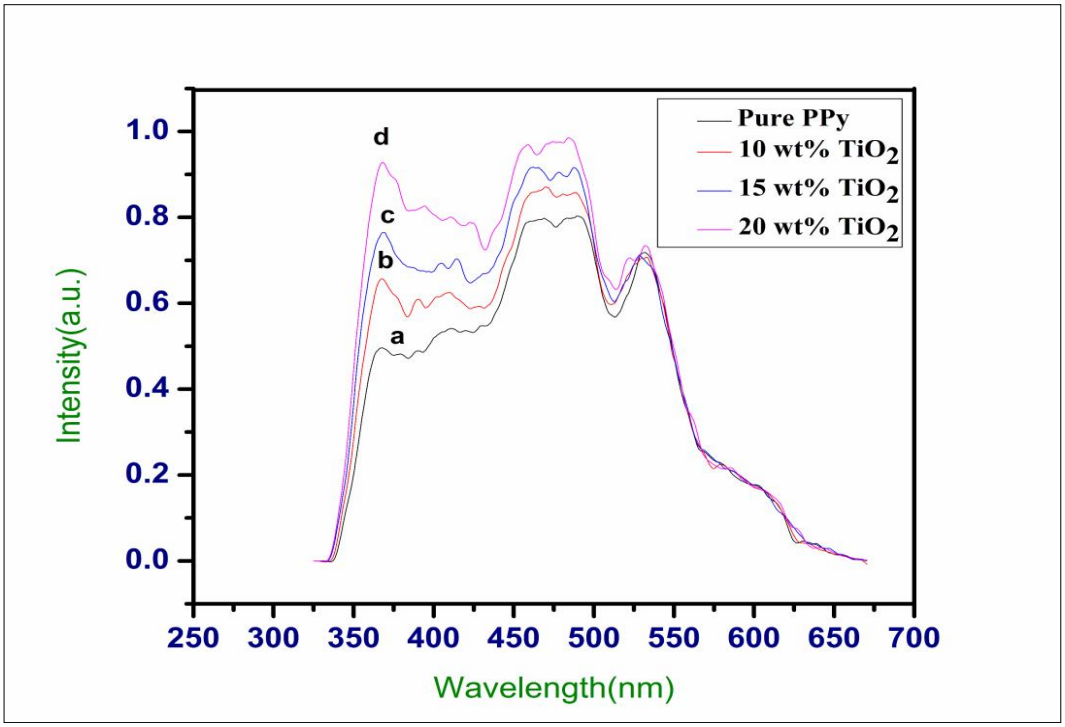

Fig 5: Photoluminescence Spectra for the Samples a, b, c and d at Room Temperature, Curves a, b, c and d Correspond to 0, 10, 15 and 20 wt% TiO_2 mixed PPy nanocomposites respectively.

3. Conclusion

In the present work pure PPy and PPy/TiO_2 doped PPy nanocomposites have been synthesized by the chemical oxidation method at temperature 5 °C. The prepared samples have been characterized by XRD, SEM, FTIR, UV-visible and PL spectroscopy. XRD spectra show the crystalline quality of all the samples, whereas the PPy synthesized is amorphous in nature. SEM micrograph shows the spherical shape nano-particle of all the samples. After incorporation of TiO_2 content in pure PPy increase the size of nanosphere. We have noticed that as the amount of TiO_2 increased the number of pores and their size also increases, that play a very important role in enhancement of photoconductivity. The study of FTIR spectra confirms the formation of conducting PPy and also suggests that doping of TiO_2 in PPy does not affect its structure. UV-visible spectra of pure PPy and PPy/TiO_2 nanocomposites sample show the absorption peak at 308nm which can be assigned to the π-π^* transition or the excitation transition. The PL spectra of 0, 10, 15 and 20 wt% TiO_2 doped PPy samples shows one emission peak centered at around 368 nm in ultra-violet region, and two broad visible peaks at around 480 nm in blue region and sharp peak at around 530 nm in green region.

4. References

1. Ramasamy RP, Veeraraghavan B, Haran B, Popov BN. J Power Sources. 2003;124:197-203.
2. Chitte HK, Bhat NV, Gore AV, Shind GN. Materials Sciences and Applications. 2011;2:1491-1498.
3. Srivastava RK, Pandey N, Mishra SK. Mater. Sci. Semiconductor. Process. 2013;16:1659-1664.
4. Kwon YJ, Kima KH, Limb CS, Shim KB. Journal of Ceramic Processing Research. 2002;3:146-149.
5. Mahmoudian MR, Basirun WJ, Alias Y, Ebadi M. Applied Surface Science. 2011;257:8317-8325.
6. Mahmoudian MR, Alias Y, Basiruna WJ, Ebadi M, Applied Surface Science. 2013;268:302-311.
7. Cullity BD. Elements of X-ray Diffraction, Addison-Wesley Publishing Company Inc., California, 1956.
8. Mahalingam T, Thanikaikarasan S, Dhanasekaran V, Mariappan R, Jayamurugan P, Velumani S. Jin-Koo Rhee, Mater. Sci. Eng. B. 2010;174:249-252.
9. Deivanayaki S, Ponnuswamy V, Mariappan R, Jayamurugan P. Optik. 2013;124:1089-1091.
10. Yang SH, Nguyen TP, Le Rendu P, Hsu CS. Compos. Part A: Appl. Sci. Manuf. 2005;36:50-513.
11. Singh SK, Verma AK, Lakhan R, Shukla RK. International Journal of Management, Information Technology and Engineering 2014;2:85-92.
12. Deivanayaki S, Ponnuswamy V, Jayamurugan P, Ashokan S. Elixir Polymer. 2012;49:10182-10185.
13. Nabid MR, Entezami AA. Journal of Applied Polymer Science. 2004;94:25-258.
14. Kim H, Change W. Synth Met. 1999;101:150-151.
15. Miquelino FLC, Paoli MAD, Genies EM. Syn. Met. 1994;68:91-96.
16. Mishra SK, Shankar SBR, Chakraborty P, Srivastava RK. Sensors and Actuators A. 2014;211:8-14.
17. Senadeera GKR, Kitamura T, Wada Y, Yanagida S. Journal of Photochemistry and Photobiology A. 2006;184:234-239.
18. Jia Y, Xiao P, He H, Yao J, Liu F, Wang Z *et al*., Applied Surface Science. 2012;258:6627-6631.